

Supplementary Information for

Curing Temperature Reduction and Performance Improvement of Solution-Processable Hole-Transporting Materials for Phosphorescent OLEDs by Manipulation of Cross-Linking Functionalities and Core Structures

*Shahid Ameen,^{‡abc} Jaemin Lee,^{‡ab} Hyun Han,^a Min Chul Suh,^{*d} and Changjin Lee^{*ab}*

^a Advanced Materials Division, Korea Research Institute of Chemical Technology, Daejeon 305-600, Republic of Korea

^b University of Science & Technology (UST), Daejeon 305-333, Republic of Korea

^c Department of Chemistry, Kohat University of Science and Technology (KUST), Kohat 26000, Pakistan

^d Department of Information Display, Kyung Hee University, Dongdaemun-gu, Seoul, 130-701, Republic of Korea

[‡] These authors contributed equally.

^{*} Corresponding author : Prof. Min Chul Suh (E-mail : mcsuh@khu.ac.kr)

^{*} Corresponding author : Dr. Changjin Lee (E-mail : cjlee@kriect.re.kr)

List of Figures

Fig. S1 (a) ^1H NMR, (b) ^{13}C NMR and (c) FAB-MS spectra of **BCzMS**.

Fig. S2 (a) ^1H NMR, (b) ^{13}C NMR and (c) FAB-MS spectra of **BCzBOS**.

Fig. S3 (a) ^1H NMR, (b) ^{13}C NMR and (c) FAB-MS spectra of **MeO-BCzBOS**.

Fig. S4 Molecular surfaces of (a) **BCzMS**, (b) **BCzBOS** and (c) **MeO-BCzBOS** by DFT calculation.

Fig. S5 Second heating scans of the cross-linkable HTL materials **BCzMS**, **BCzBOS** and **MeO-BCzBOS**.

Fig. S6 UV-Vis. absorption spectra of thermally cross-linked **BCzMS** films before and after solvent rinsing with different thermal curing temperatures.

Fig. S7 UV-Vis. absorption spectra of thermally cross-linked **BCzBOS** films before and after solvent rinsing, with different thermal curing temperatures.

Fig. S8 UV-Vis. absorption spectra of thermally cross-linked **MeO-BCzBOS** films before and after solvent rinsing, with different thermal curing temperatures.

Fig. S9 Electroluminescence spectra of the HTL-containing OLED devices.

Fig. S10 Luminance-Voltage characteristics of OLEDs by changing the thermal curing temperatures of (a) **BCzBOS** and (b) **BCzMS**.

Fig. S11 Optical microscope images of the (a) **BCzBOS** and (b) **MeO-BCzBOS** HTL films.

Fig. S12 AFM analysis results of the HTL films.

Fig. S13 External quantum efficiency graph of the HTL-containing OLED devices.

Fig. S14 Energy levels diagram for the devices.

(c)

[Mass Spectrum]
Data : 3-8-003 Date : 08-Mar-2016 10:29
Sample: MS
Note : NDR
Inlet : Direct Ion Mode : FRR+
Spectrum Type : Normal Ion (MF-Linear)
RT : 0.17 min Scan# : 2
BP : m/z 154.0000 Int. : 302.00
Output m/z range : 100.0000 to 852.9574 Cut Level : 0.70 %

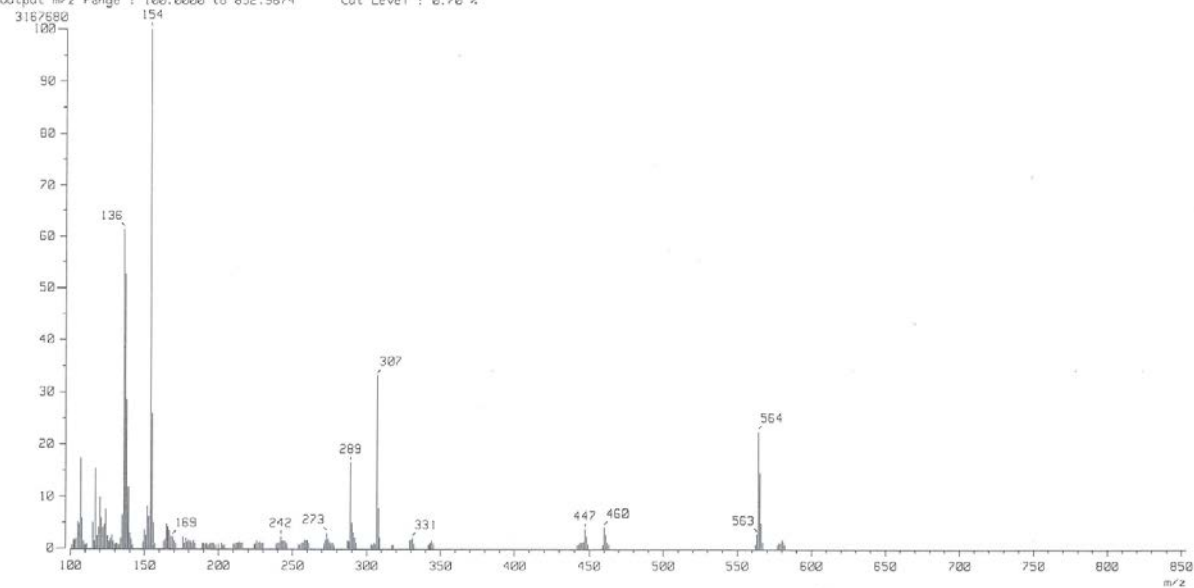
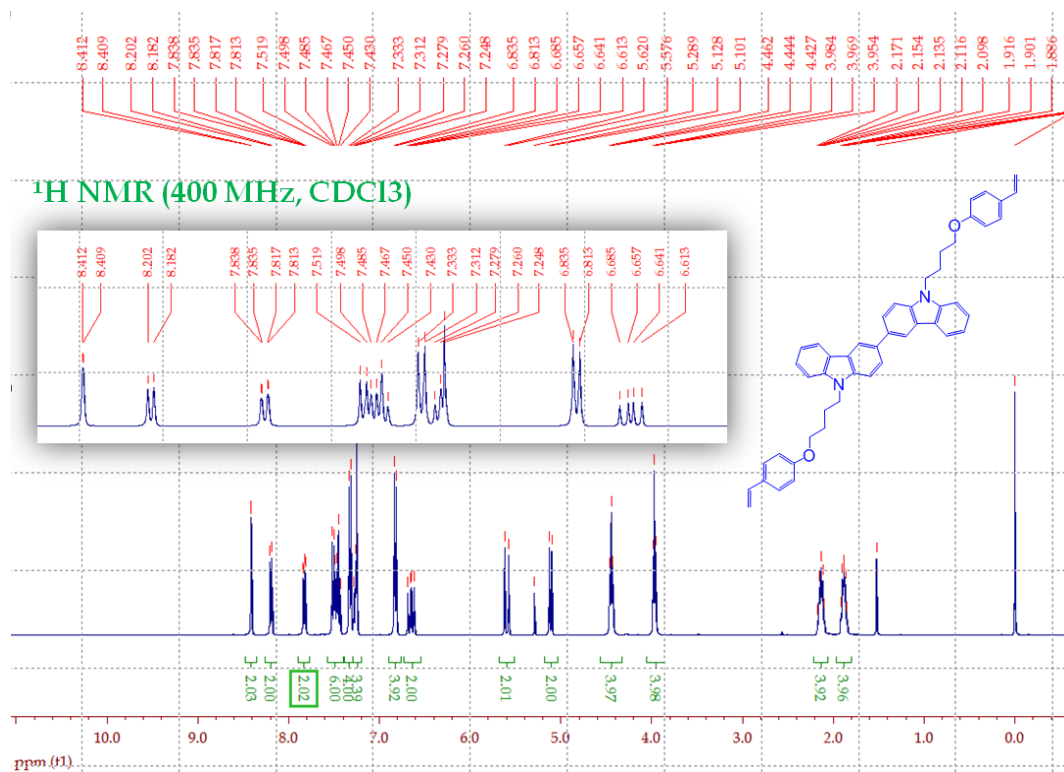
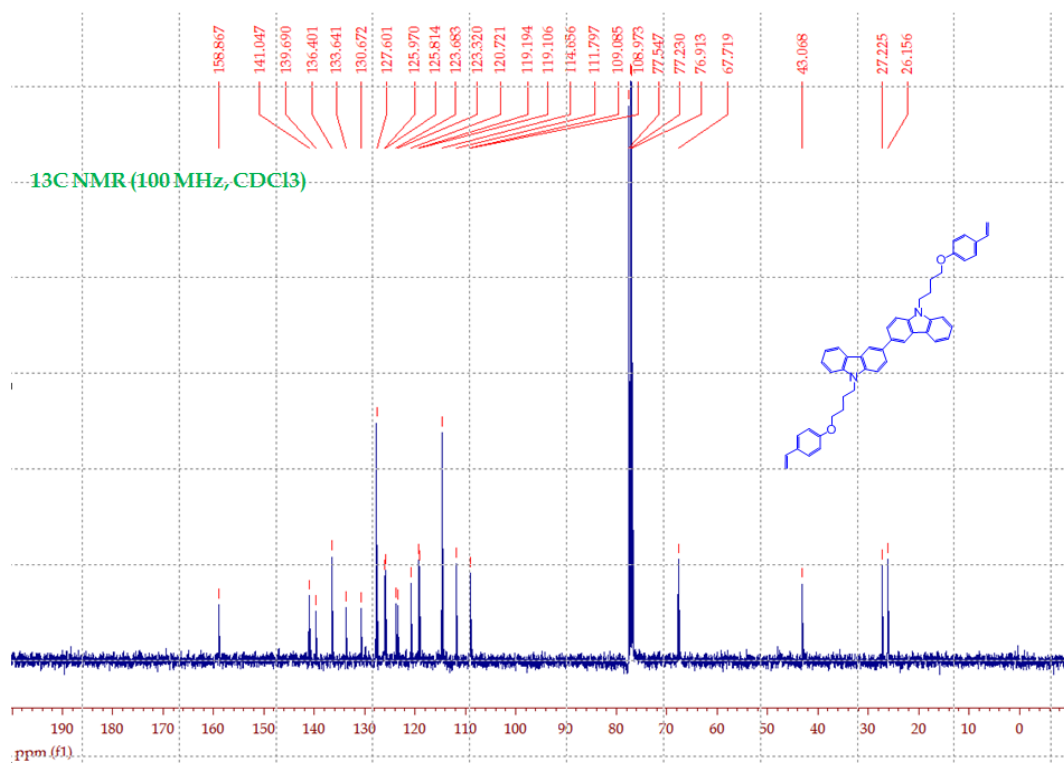


Fig. S2 (a) ^1H NMR, (b) ^{13}C NMR and (c) FAB-MS spectra of BCzBOS.

(a)



(b)



(c)

[Mass Spectrum]
Data : 3-8-003 Date : 08-Mar-2016 10:29
Sample: MS
Note : NDR
Inlet : Direct Ion Mode : FRR+
Spectrum Type : Normal Ion (MF-Linear)
RT : 0.17 min Scan# : 2
BP : m/z 154.0000 Int. : 302.00
Output m/z range : 100.0000 to 852.9574 Cut Level : 0.70 %

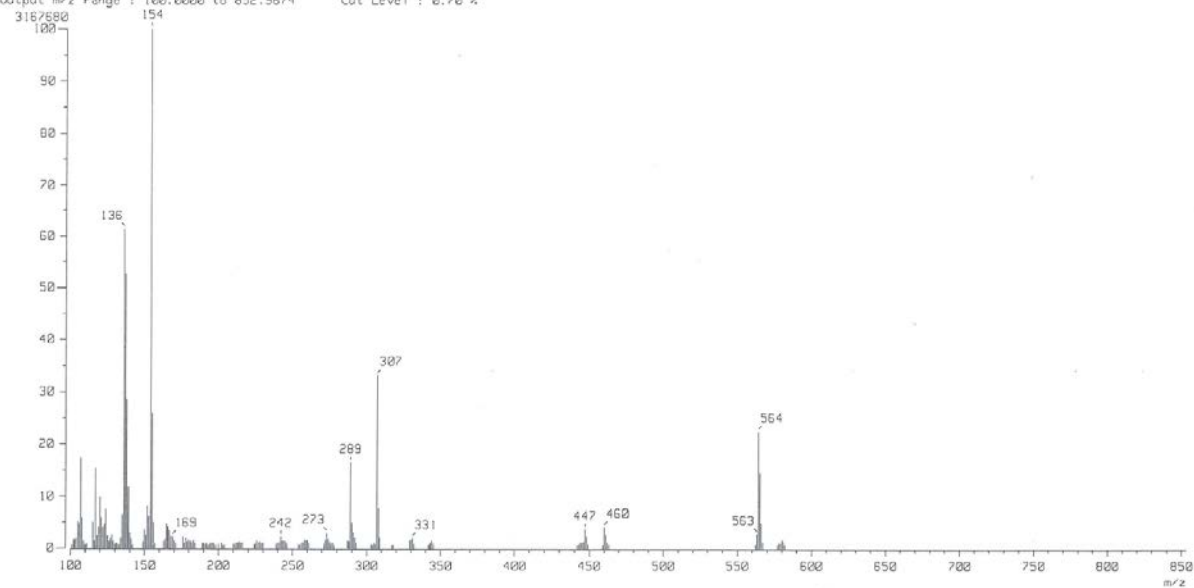
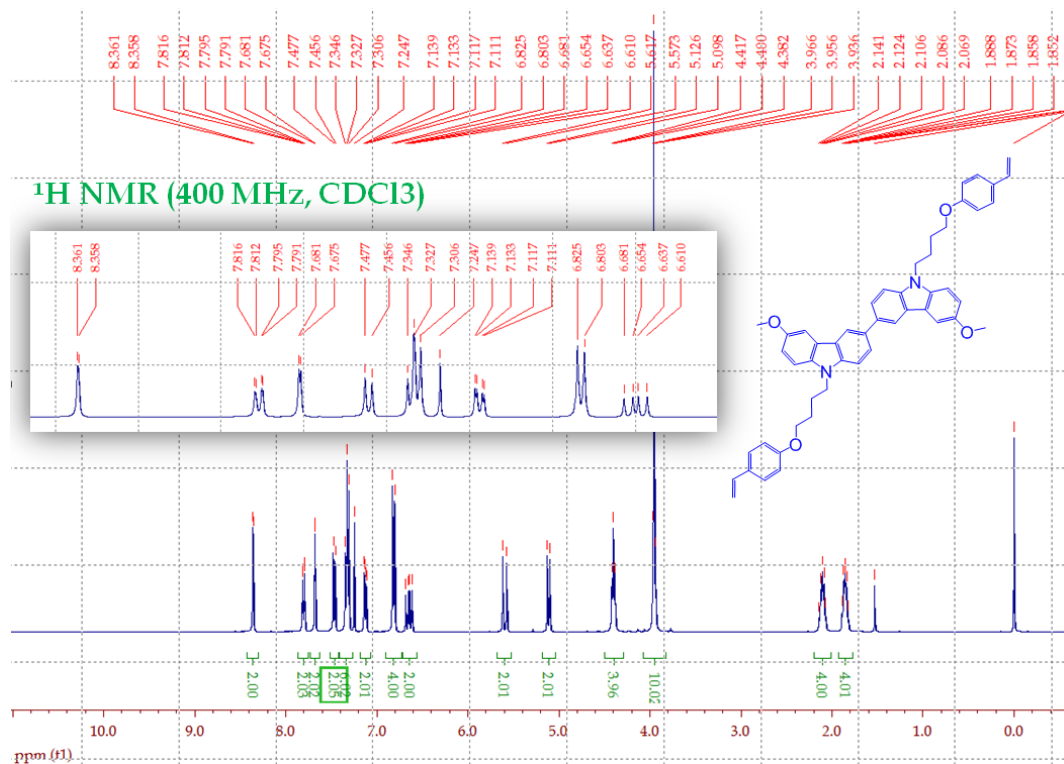
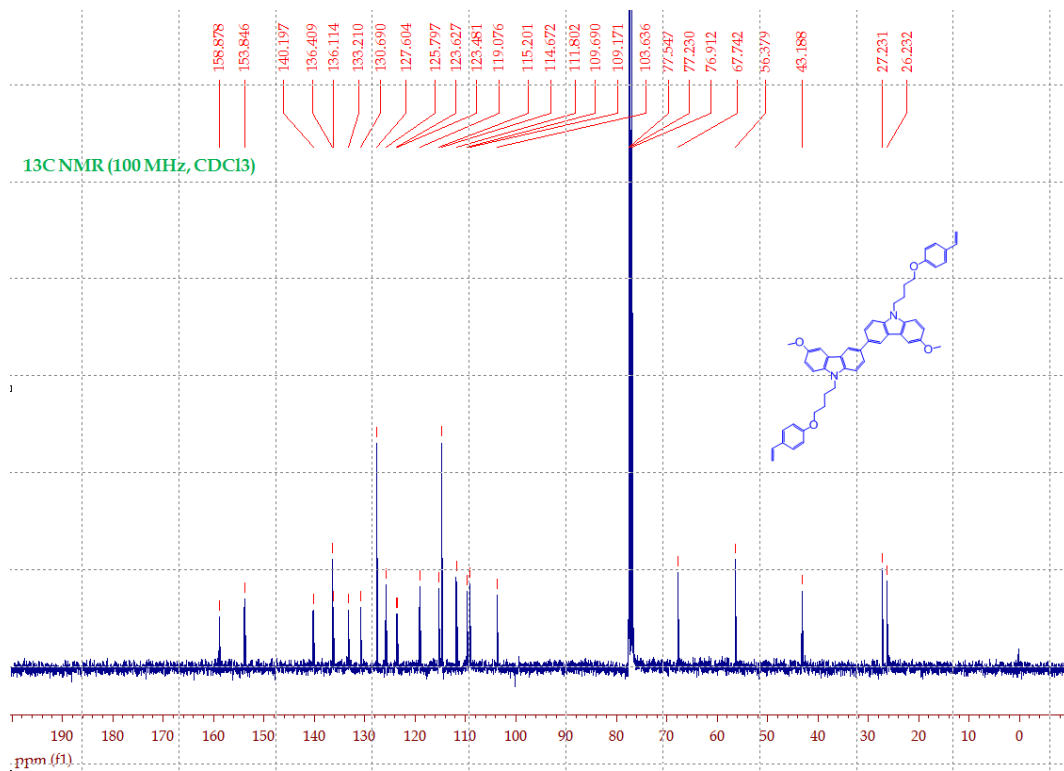


Fig. S3 (a) ^1H NMR, (b) ^{13}C NMR and (c) FAB-MS spectra of MeO-BCzBOS.

(a)



(b)



(c)

[Mass Spectrum]
Data : 3-8-003 Date : 08-Mar-2016 10:29
Sample: MS
Note : NDR
Inlet : Direct Ion Mode : FRR+
Spectrum Type : Normal Ion (MF-Linear)
RT : 0.17 min Scan# : 2
BP : m/z 154.0000 Int. : 302.00
Output m/z range : 100.0000 to 852.9574 Cut Level : 0.70 %

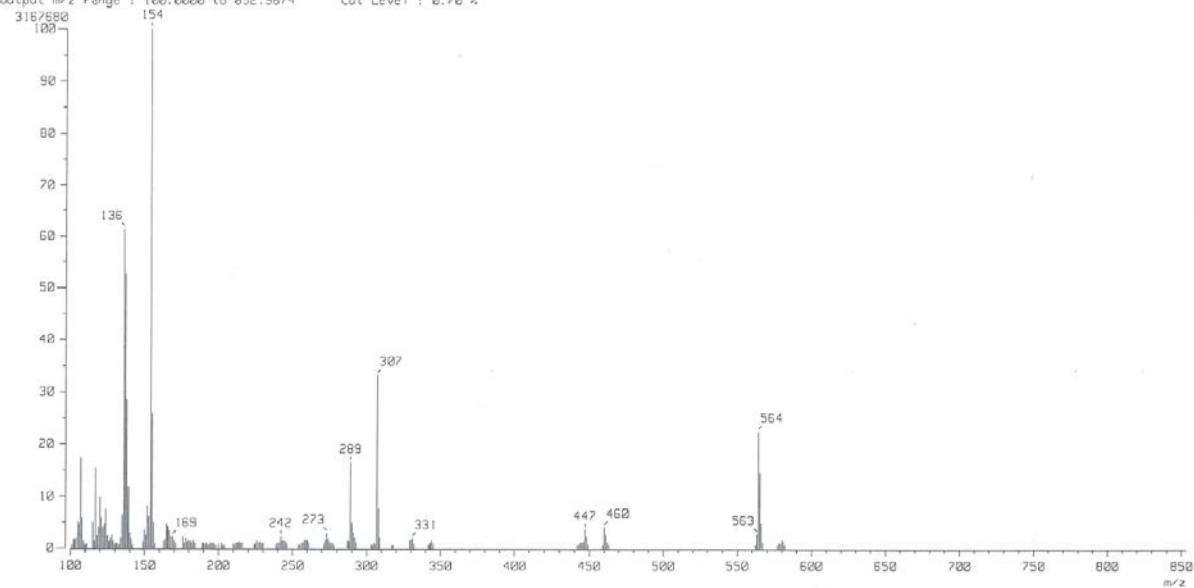
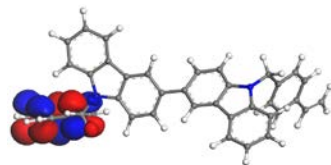


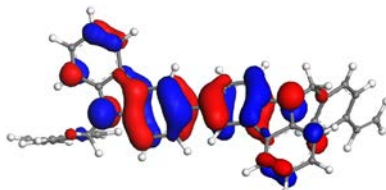
Fig. S4 Molecular surfaces of (a) **BCzMS**, (b) **BCzBOS** and (c) **MeO-BCzBOS** by DFT calculation.

(a)

LUMO
(-1.25 eV)

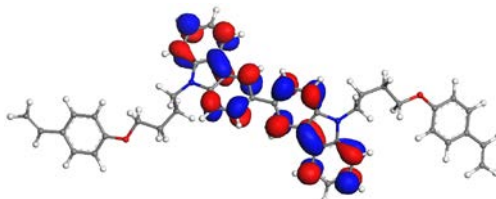


HOMO
(-5.19 eV)

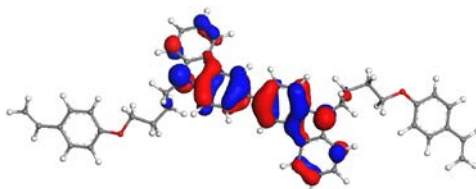


(b)

LUMO
(-0.99 eV)

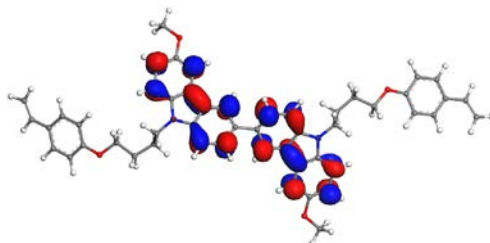


HOMO
(-5.28 eV)



(c)

LUMO
(-1.03 eV)



HOMO
(-4.96 eV)

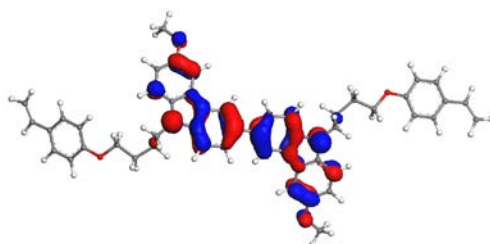


Fig. S5 Second heating scans of the cross-linkable HTL materials **BCzMS**, **BCzBOS** and **MeO-BCzBOS**

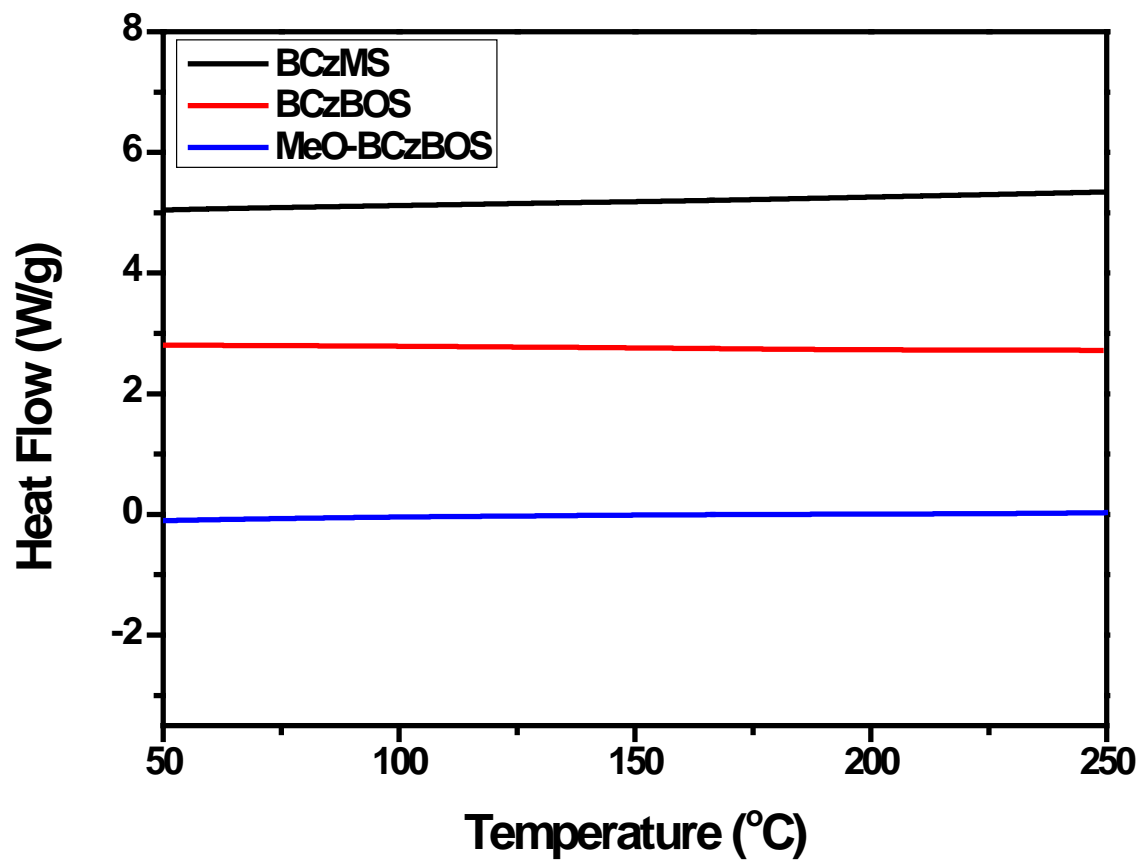
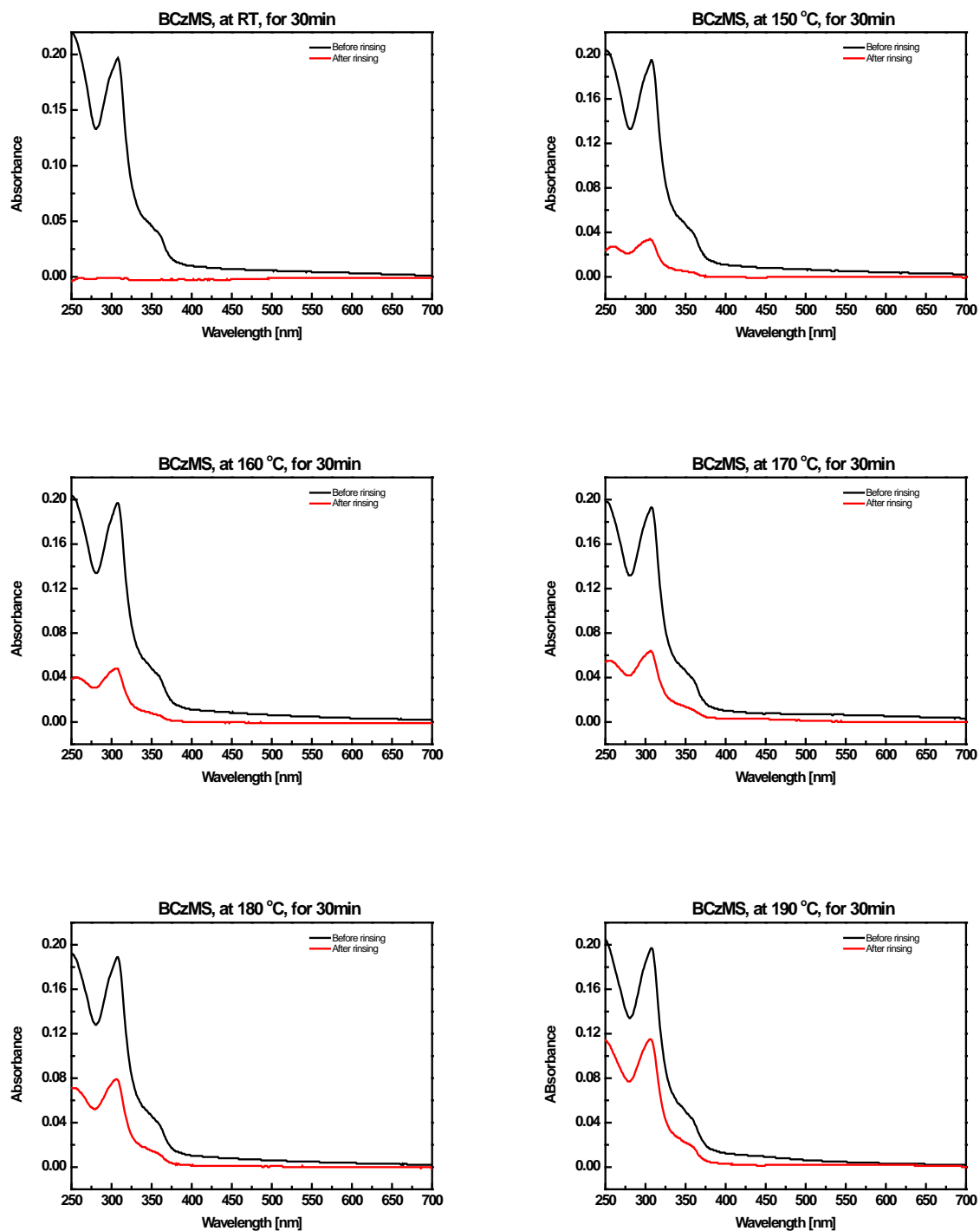


Fig. S6 UV-Vis. absorption spectra of thermally cross-linked **BCzMS** films before and after solvent rinsing with different thermal curing temperatures.



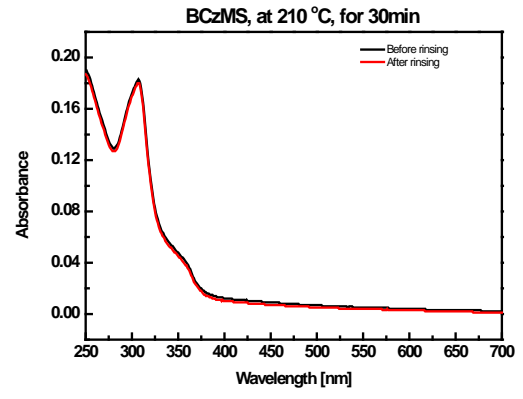
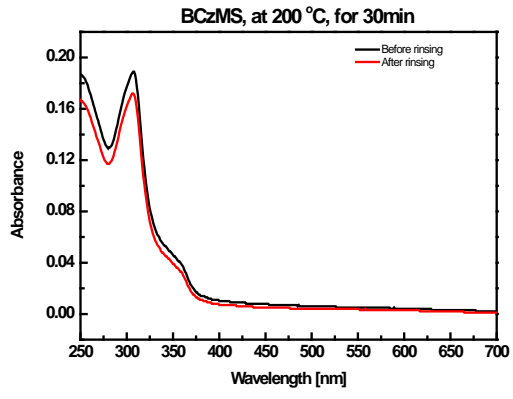
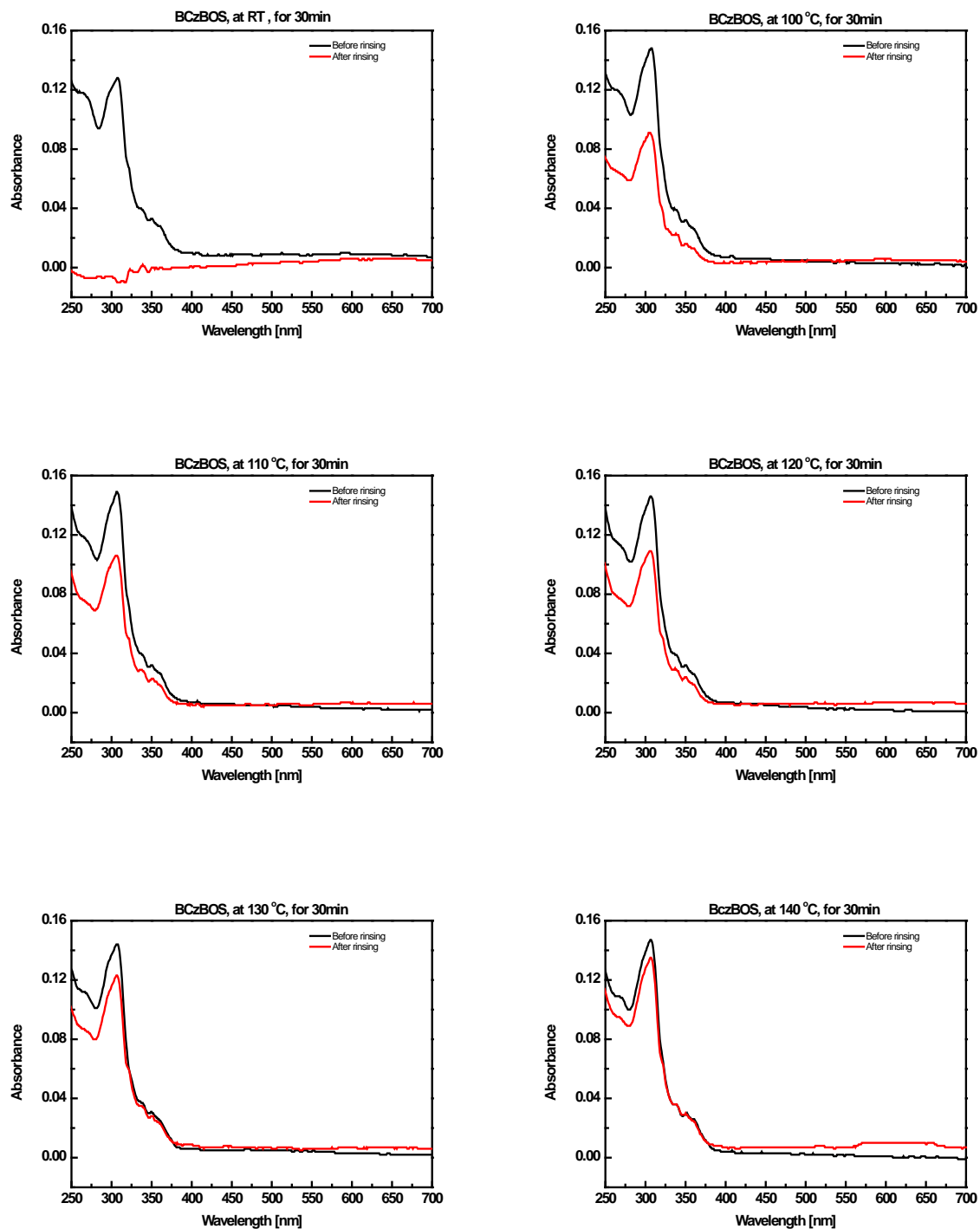


Fig. S7 UV-Vis. absorption spectra of thermally cross-linked **BCzBOS** films before and after solvent rinsing with different thermal curing temperatures.



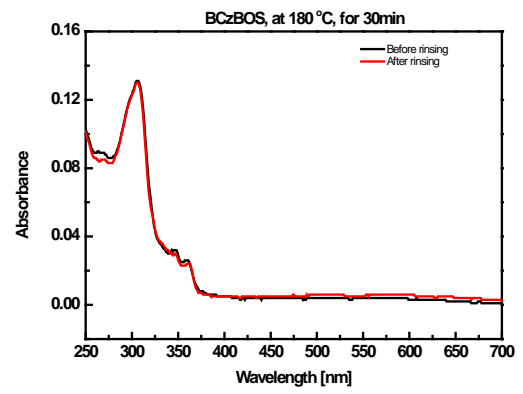
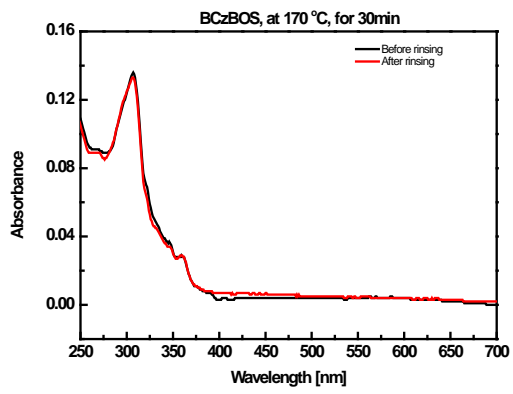
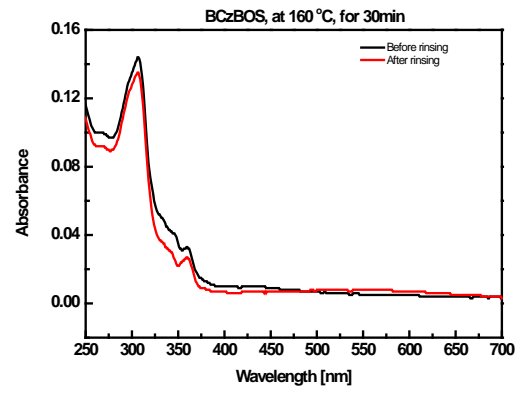
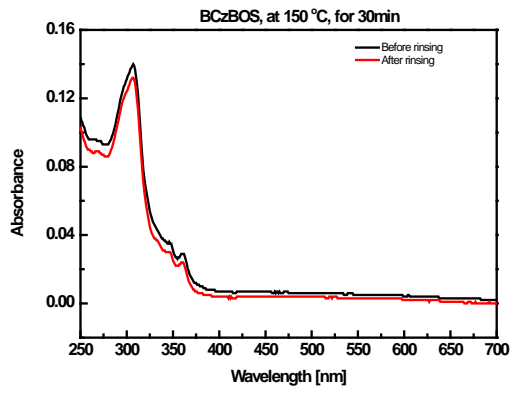
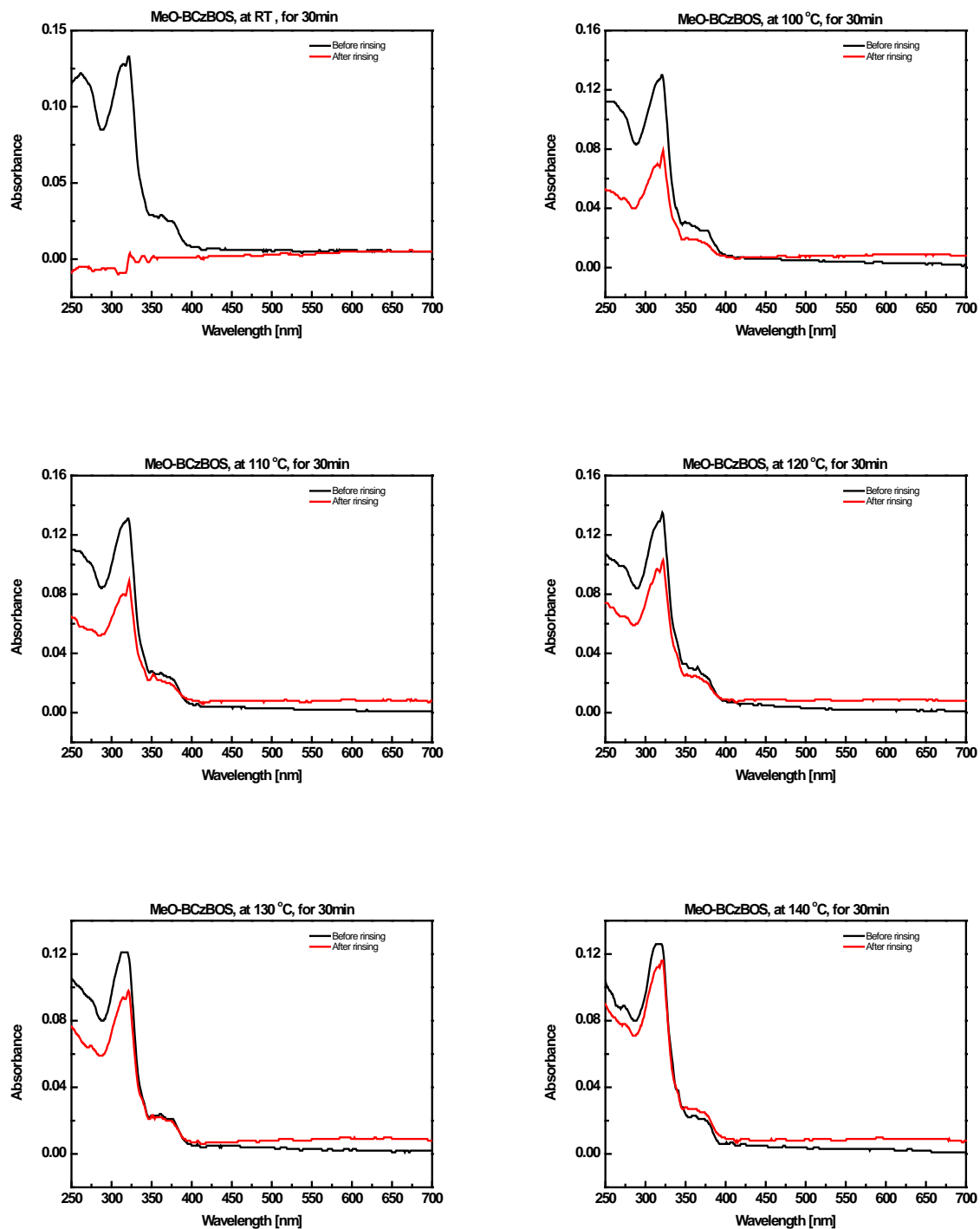


Fig. S8 UV-Vis. absorption spectra of thermally cross-linked **MeO-BCzBOS** films before and after solvent rinsing with different thermal curing temperatures.



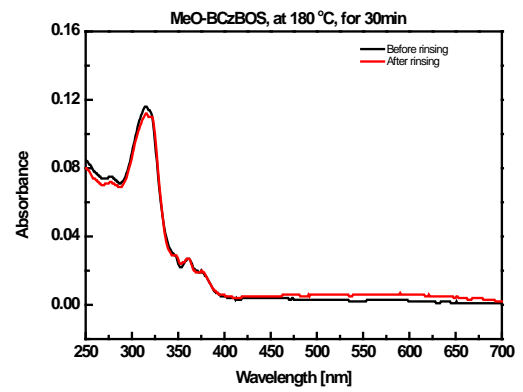
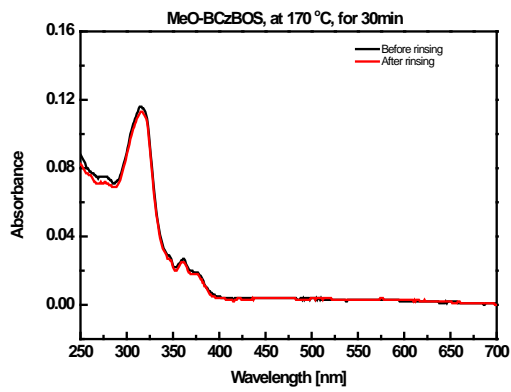
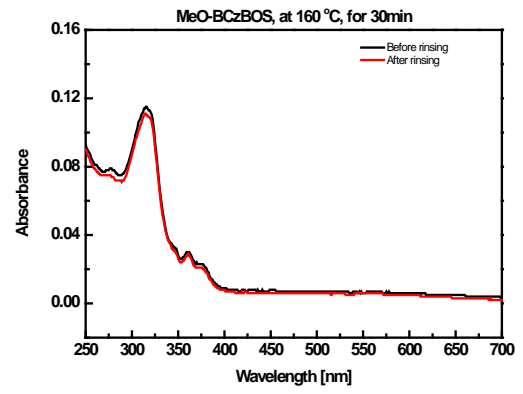
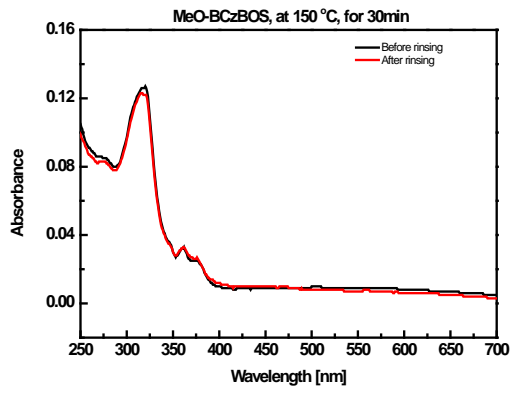


Fig. S9 Electroluminescence spectra of the HTL-containing OLED devices.

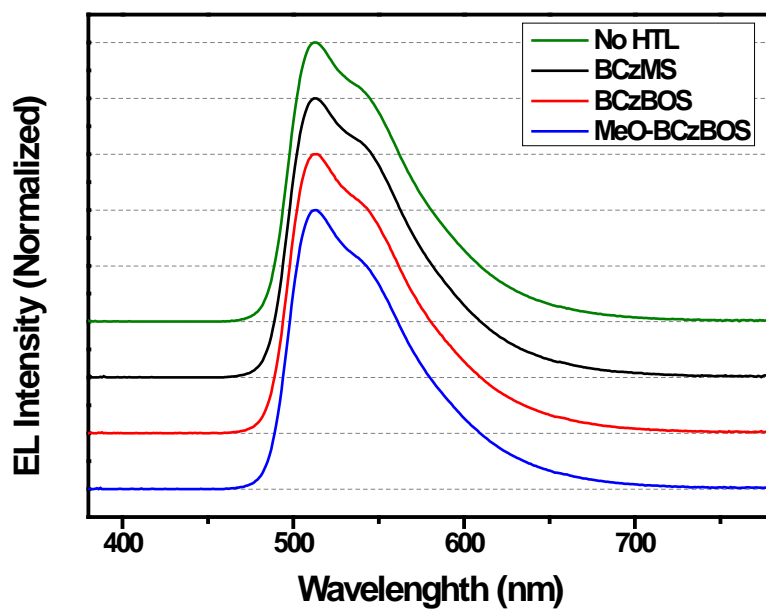
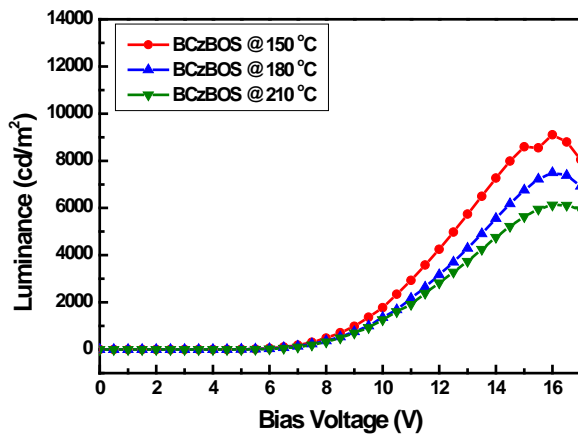


Fig. S10 Luminance-Voltage characteristics of OLEDs by changing the thermal curing temperatures of (a) **BCzBOS** and (b) **BCzMS**.

(a)



(b)

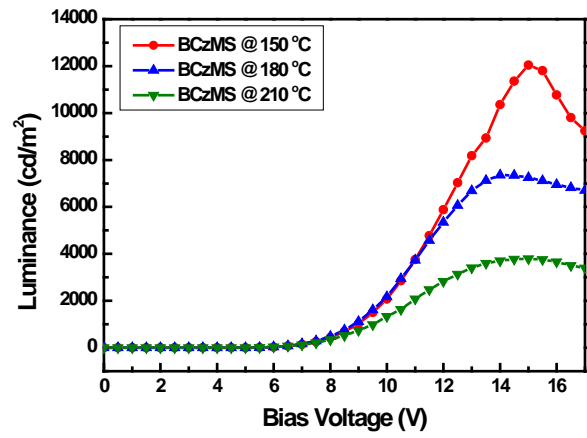
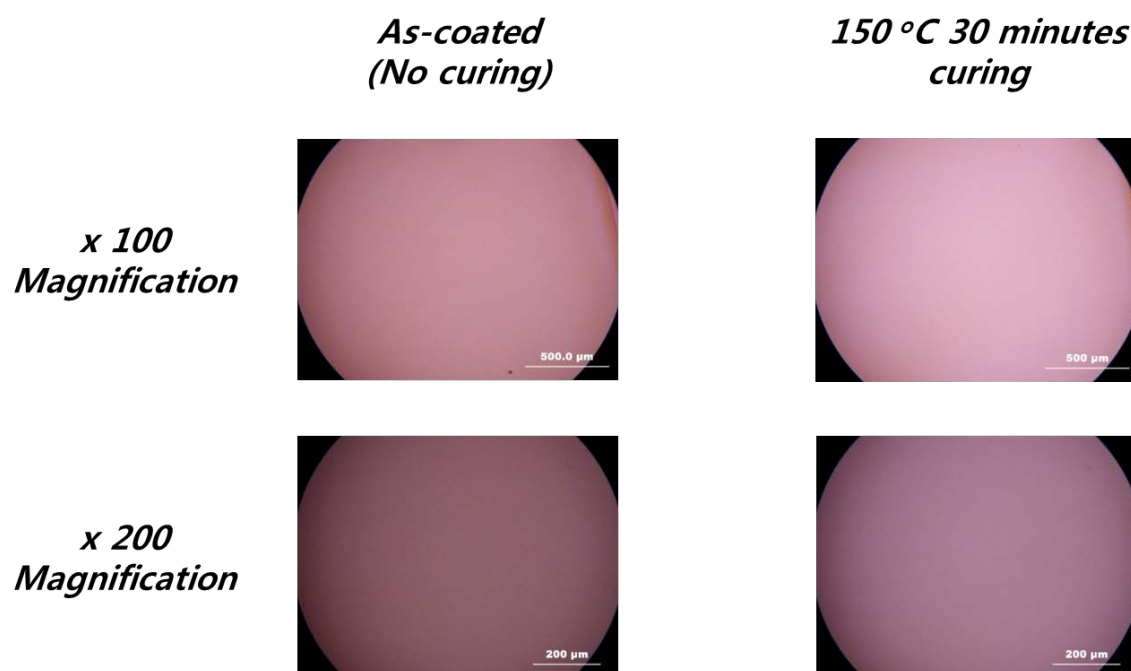


Fig. S11 Optical microscope images of the (a) **BCzBOS** and (b) **MeO-BCzBOS** HTL films.

(a)



(b)

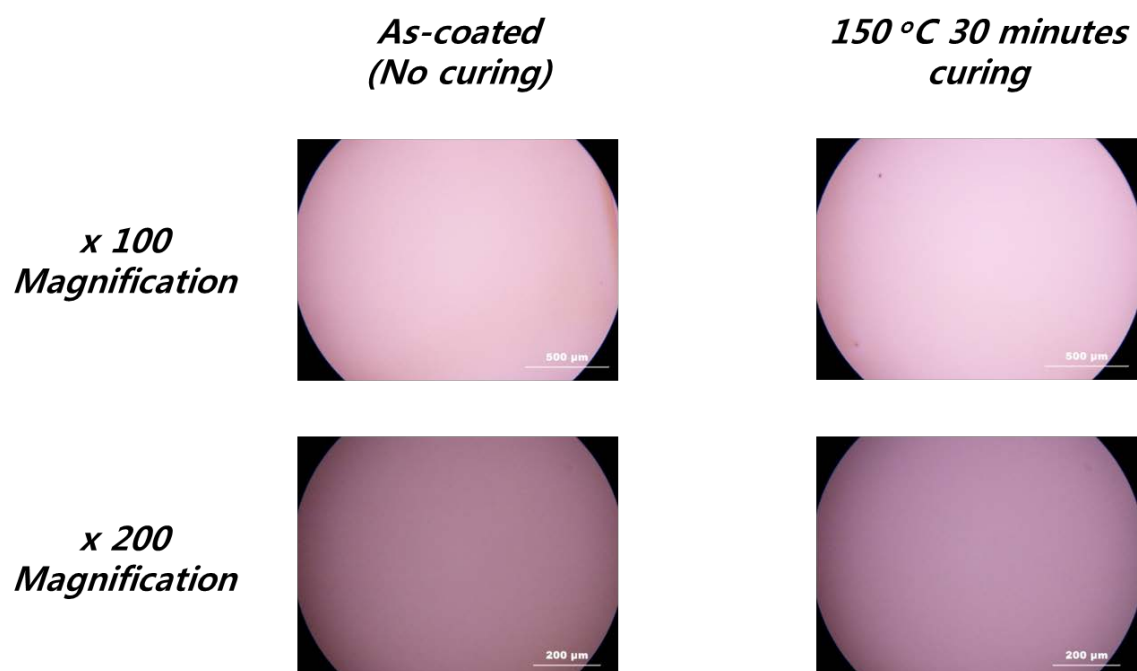
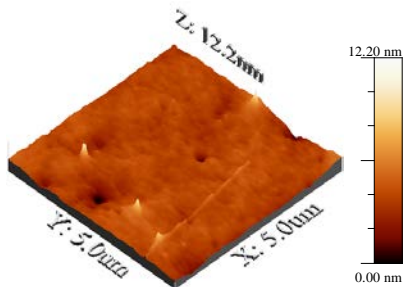
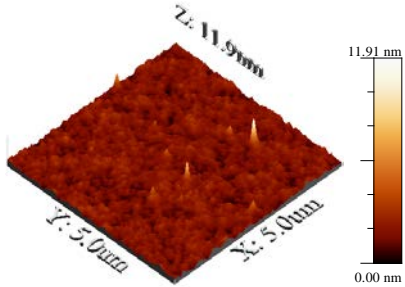
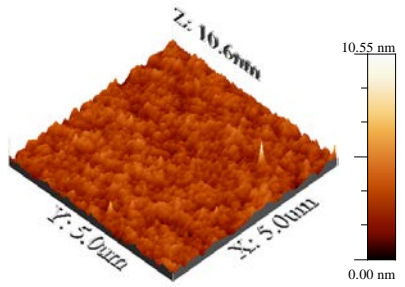
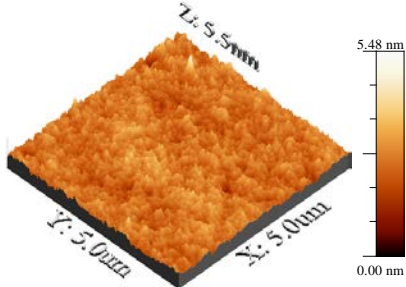
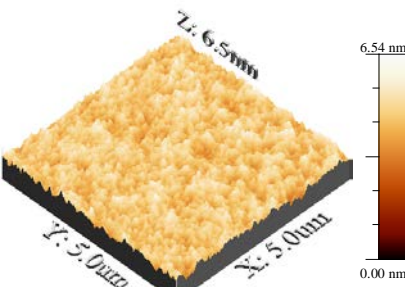
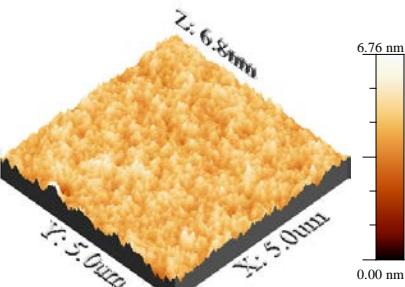
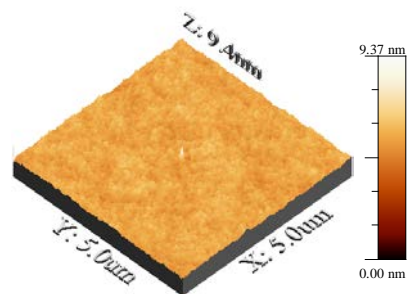


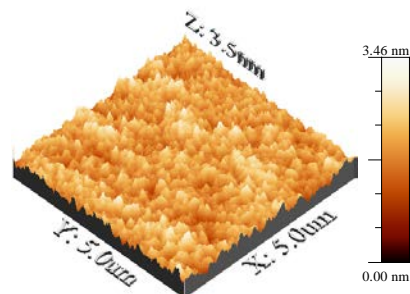
Fig. S12 AFM analysis results of the HTL films.

	Before curing	After curing	After washing
BCzMS	 <p>RMS roughness : 0.62 nm</p>	 <p>RMS roughness : 0.56 nm</p>	 <p>RMS roughness : 0.75 nm</p>
BCzBOS	 <p>RMS roughness : 0.40 nm</p>	 <p>RMS roughness : 0.49 nm</p>	 <p>RMS roughness : 0.52 nm</p>

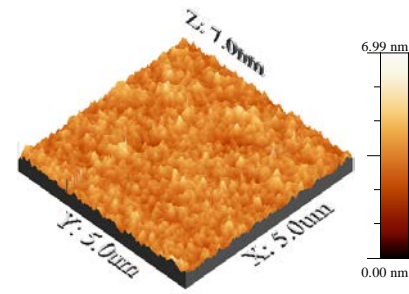
MeO-BCzBOS



RMS roughness : 0.34 nm



RMS roughness : 0.36 nm



RMS roughness : 0.50 nm

Fig. S13 External quantum efficiency graph of the HTL-containing OLED devices.

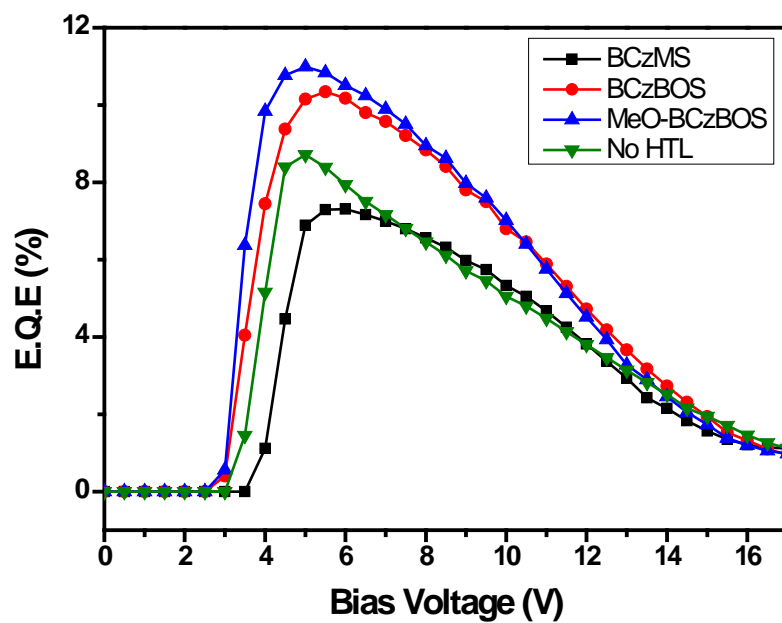


Fig. S14 Energy levels diagram for the devices.

